Journal of Non-Crystalline Solids 426 (2015) 137–140

Contents lists available at ScienceDirect

Journal of Non-Crystalline Solids

journal homepage: www.elsevier.com/ locate/ jnoncrysol

Atomic-scale structural heterogeneity and elastic modulus for metallic glasses

Haishun Liu [a], Qingling Liu [a], Hai Su [a], Weiming Yang [a,b,*], Yucheng Zhao [a], Juntao Huo [b], Baolong Shen [c]

[a] School of Sciences, School of Mechanics and Civil Engineering, State Key Laboratory for Geomechanics and Deep Underground Engineering, China University of Mining and Technology, Xuzhou 221116, China
[b] Zhejiang Province Key Laboratory of Magnetic Materials and Application Technology, Key Laboratory of Magnetic Materials and Devices, Ningbo Institute of Materials Technology & Engineering, Chinese Academy of Sciences, Ningbo 315201, China
[c] School of Materials Science and Engineering, Southeast University, Nanjing 211189, China

ARTICLE INFO

Article history:
Received 22 May 2015
Received in revised form 4 July 2015
Accepted 6 July 2015
Available online 15 July 2015

Keywords:
Metallic glasses;
Microstructure;
Elastic modulus;
Atomic-scale structural heterogeneity

ABSTRACT

The role of atomic-scale structural heterogeneity (ASSH) in the elastic modulus for metallic glasses (MGs) is investigated. A strategy for estimating the strength of ASSH in MGs is proposed and then the fraction of ASSH is obtained. It is found that the fraction of ASSH could be the basic entities responsible for the change of elastic modulus during the change of composition and structure relaxation in MGs.

1. Introduction

As promising functional and structural materials, metallic glasses (MGs) possess excellent mechanical, magnetic, and chemical properties; and these unique properties are believed to be closely related to their disordered atomic structures [1–3]. It is, therefore, essential to study this disordered structure for better understanding and then tailoring these materials with desired properties [4]. Although MGs are isotropic and homogeneous on macroscale, recent studies have found the existence of the loose or weakly bound atoms in the oversized cages, voids, or similar defects, named as atomic-scale structural heterogeneity (ASSH) [5] besides short- and medium-range order clusters [6]. Such microstructure may affect the elastic deformation of MGs as well [7]. Some of the studies also suggest that the elastic deformation in MGs mainly occurs at solvent–solvent junctions among solute-centered clusters; and the elastic modulus is essentially determined by solvent–solvent bonding [8,9]. However, extensive experiments illustrate that the elastic modulus is very sensitive to the minor change of composition which may lead to the appearance of ASSH in MGs [10]. This induces the following interesting question: how does the ASSH affect the elastic modulus of MGs? It has been proven that the excess low frequency vibrational contribution appears as a bump in $C_{p,Latt}/T^3$–T curves ($C_{p,Latt}$ is the lattice specific heat and T is the temperature), which is significantly affected by structural heterogeneity in MGs [11–13]. Thus, the study of the excess low frequency vibrations may help understand the role of ASSH in elastic modulus for MGs. In this paper, we study $(Fe_{1-x}Co_x)_{72}B_{20}Si_4Nb_4$ ($x = 0.1$, 0.3, 0.5, and 0.7) to investigate the role of ASSH in elastic modulus for MGs. It will provide guidance for the substitution of an element for varying mechanical properties in MGs.

2. Experimental

$(Fe_{1-x}Co_x)_{72}B_{20}Si_4Nb_4$ ($x = 0.1$, 0.3, 0.5 and 0.7) and $(Fe_{0.5}Co_{0.5})_{72}B_{20}Si_4Nb_4$ MGs are prepared by arc melting the mixture of Fe (99.99%), Co (99.99%), Nb (99.99%) metals and B (99.50%), Si (99.99%) crystals in an argon atmosphere, $(Fe_{0.5}Co_{0.5})_{72}B_{20}Si_4Nb_4$ MG is annealed at 823, 873, and 923 K for 0.5 h in vacuum. Cylindrical alloy rods are produced by copper mold casting method [14]. The glassy nature is ascertained by X-ray diffraction (XRD), differential scanning calorimeter (DSC) and transmission electron microscopy (TEM). The isobaric low temperature specific heat C_p of as-cast $(Fe_{1-x}Co_x)_{72}B_{20}Si_4Nb_4$ ($x = 0.1$, 0.3, 0.5, and 0.7) MGs and annealed $(Fe_{0.5}Co_{0.5})_{72}B_{20}Si_4Nb_4$ metallic glass (MG) are measured by the Physical Property Measurement System (PPMS6000) with disk shape (~0.5 mm in thickness). The relative error for the specific heat measurements is less than 2%. Elastic modulus is measured using ultrasonic method. The rods (~3.0 mm) are cut to 6.0–

* Corresponding author at: School of Sciences, School of Mechanics and Civil Engineering, State Key Laboratory for Geomechanics and Deep Underground Engineering, China University of Mining and Technology, Xuzhou 221116, China.
E-mail address: wmyang@cumt.edu.cn (W. Yang).

http://dx.doi.org/10.1016/j.jnoncrysol.2015.07.016
0022-3093/

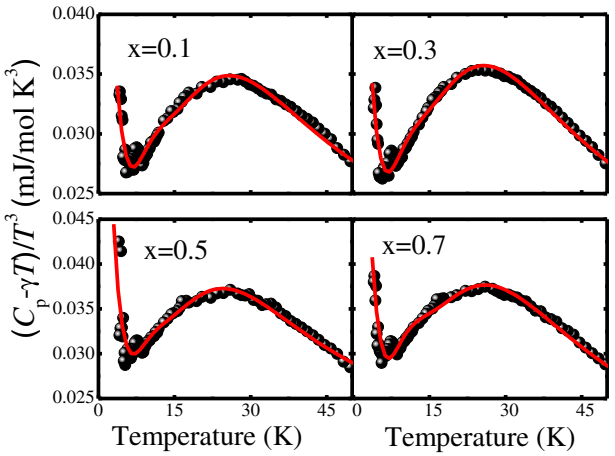

Fig. 1. Standard plotting of $(C_p - \gamma T) / T^3$ versus T for $(Fe_{1-x}Co_x)_{72}B_{20}Si_4Nb_4$ ($x = 0.1, 0.3, 0.5$ and 0.7) MGs. The fitting lines from experimental data with Eq. (3) are also shown.

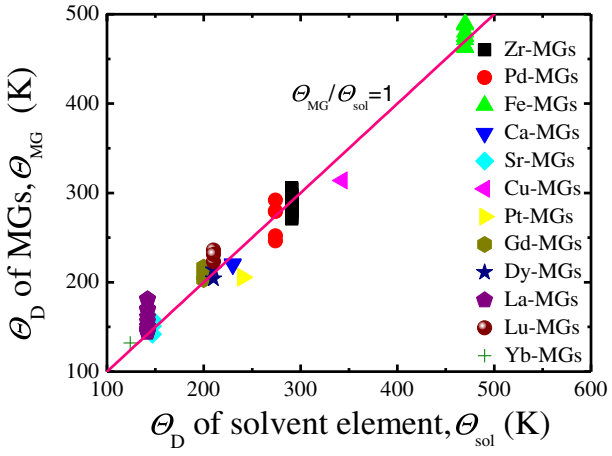

Fig. 2. The average ratio of θ_D for various MGs and their solvent. Data are taken from Ref. [18,23].

8.0 mm in length and their ends are carefully polished flat and parallel. The acoustic longitudinal and transverse velocities are measured using pulse echo overlap method by a MATEC 6600 model ultrasonic system [9]. The final data were obtained by averaging 3 experimental results. The relative error for the ultrasonic measurements is less than 5%. The densities of the specimens are measured using Archimedes's method with an accuracy of about 2%.

3. Results and discussion

Fig. 1 exhibits $(C_p - \gamma T) / T^3$ vs T for $(Fe_{1-x}Co_x)_{72}B_{20}Si_4Nb_4$ ($x = 0.1$, 0.3, 0.5, and 0.7) MGs, where, C_p is the low temperature specific heat, and γ is the electronic specific heat coefficient with values 6.96, 6.26, 5.92, and 5.72 mJ/mol K^2 for $(Fe_{1-x}Co_x)_{72}B_{20}Si_4Nb_4$ ($x = 0.1$, 0.3, 0.5, and 0.7) MGs, respectively, depending linearly on the temperature [15]. From Fig. 1, it can be seen that there exists excess peaks of specific heat in 10–50 K temperature regions in the metallic glassy systems.

According to the solid state theory, the low temperature specific heat C_p can be assumed to be consisted of three terms

$$C_p = C_e + C_M + C_L \tag{1}$$

where $C_e = \gamma T$ represents the electronic contribution to C_p, $C_M = \delta T^{3/2}$ the magnetic contribution [16], and C_L the lattice specific heat, which originates from the Debye oscillator and Einstein oscillators. Here Einstein oscillators are mainly responsible for ASSH in MGs, such as the loose or weakly bound atoms in the oversized cages, voids, or similar defects in the case of complex materials [17]. It seems that the experimental curves presented in Fig. 1 have two minimums, which mean that two distinct Einstein-type vibration modes exist in the MGs [15]. However, the second Einstein-type vibration mode is relatively small [19], and then it can be ignored in this work. Then, the lattice specific heat C_L can be expressed as

$$C_L = (1-f)C_D + fC_E \tag{2}$$

where f is the fraction of ASSH in the glassy state; $C_D = 3R(\frac{T}{\theta_D})^3 \int_0^{\theta_D/T} \frac{\xi^4 e^\xi}{(e^\xi-1)^2} d\xi$, the contribution of Debye term, with θ_D the Debye temperature; and $C_E = R(\frac{\theta_E}{T})^2 \frac{e^{\theta_E/T}}{(e^{\theta_E/T}-1)^2}$, the contribution of Einstein mode, with θ_E the Einstein temperature, and R the gas constant.

Then the relationship between $(C_p - \gamma T) / T^3$ and T can be drawn as

$$\frac{C_p-\gamma T}{T^3} \approx \frac{234R(1-f)}{\theta_D^3} + \frac{fR\theta_E^2}{T^5}\frac{e^{\theta_E/T}}{(e^{\theta_E/T}-1)^2} + \delta T^{-3/2}. \tag{3}$$

The comparisons of theoretical values and experimental data of $(C_p - \gamma T) / T^3$ vs T for $(Fe_{1-x}Co_x)_{72}B_{20}Si_4Nb_4$ ($x = 0.1$, 0.3, 0.5, and 0.7) MGs are also shown in Fig. 1. It can be seen that the theoretical lines are consistent with the experiments. The values of Debye temperature θ_D, Einstein temperature θ_E and magnetic specific heat coefficient δ obtained from the least-squares fit of the present data to Eq. (3) are summarized in Table 1. The presence of the relatively large δ coefficient means a substantial deviation of magnetic ions from the lattice specific heat C_L, occurring at relatively low temperatures for $(Fe_{1-x}Co_x)_{72}B_{20}Si_4Nb_4$ MGs. It can be also seen from Table 1 that the ratio of θ_D to θ_E is around 5. These results are in good agreement with Ref. [19]. The expression of θ_D and θ_E can be unified as

$$\theta_i = \frac{\hbar\omega_i}{k_B} \tag{4}$$

Table 1
Terms from fits to Eq. (3) for the low temperature specific heat of $(Fe_{1-x}Co_x)_{72}B_{20}Si_4Nb_4$ ($x = 0.1$, 0.3, 0.5 and 0.7) MGs. The Debye temperatures of solvent components are also listed.

Metallic glasses	Base metal	θ_D[a]	θ_D (K)	θ_E (K)	δ (mJ/mol K$^{5/2}$)
$(Fe_{0.9}Co_{0.1})_{72}B_{20}Si_4Nb_4$	Fe	470	480 ± 10	90 ± 5	0.103
$(Fe_{0.7}Co_{0.3})_{72}B_{20}Si_4Nb_4$	Fe	470	475 ± 5	93 ± 3	0.116
$(Fe_{0.5}Co_{0.5})_{72}B_{20}Si_4Nb_4$	Fe/Co	470/445	460 ± 10	95 ± 5	0.147
$(Fe_{0.3}Co_{0.7})_{72}B_{20}Si_4Nb_4$	Co	445	450 ± 15	100 ± 5	0.165

[a] Reference [18].

Table 2
Elastic moduli of MGs from experiments and the prediction in the present work. Also listed are the elastic moduli of solvents and the fraction of ASSH in the glassy state for several MGs.

Metallic glasses	f (%)	E_{Sol}[a] (GPa)	E_{Cal} (GPa)	E_{Exp} (GPa)	G_{Sol}[a] (GPa)	G_{Cal} (GPa)	G_{Exp} (GPa)	Ref
$(Fe_{0.9}Co_{0.1})_{72}B_{20}Si_4Nb_4$	2.6	211	204	–	82	79	–	This work
$(Fe_{0.7}Co_{0.3})_{72}B_{20}Si_4Nb_4$	3.9	211	201	192 ± 9	82	78	68 ± 3	This work
$(Fe_{0.5}Co_{0.5})_{72}B_{20}Si_4Nb_4$	4.3	211	200	195 ± 9	82	78	70 ± 4	This work
$(Fe_{0.3}Co_{0.7})_{72}B_{20}Si_4Nb_4$	3.5	209	200	200 ± 10	–	–	80 ± 4	This work
$Cu_{50}Zr_{50}$	8.4	98	88	85	35	32	31	[23,24]
$Pd_{41.25}Cu_{41.25}P_{17.5}$	6.0	121	112	105	44	41	37	[23,25]
$Pd_{40}Cu_{30}Ni_{10}P_{20}$	2.3	121	117	102	44	43	36	[26,27]
$Zr_{46.75}Ti_{8.25}Cu_{7.5}Ni_{10}Be_{27.5}$	5.0	98	93	100	35	33	37	[11,17]
$Zr_{52.5}Ti_5Cu_{17.9}Ni_{14.6}Al_{10}$	4.3	98	93	89	35	33	32	[13,27]

[a] Reference [18].

where $\hbar$ is the reduced Planck constant, ω_i $(i = D, E)$ the vibration frequency of Debye oscillator and Einstein oscillator respectively, and k_B the Boltzmann constant.

Similarly, the vibration frequency in MGs is expressed based on the simple harmonic vibration model as [20]

$$\omega_i = \sqrt{\frac{k_i}{m_i}} \tag{5}$$

where k_i $(i = D, E)$ is the restoring force of interatomic bonds, and m_i $(i = D, E)$ the mass of the oscillator. Considering $m_D \approx m_E$, we obtain that the k_D of MGs is almost equal to their base elements, and the ratio k_E/k_D is drawn about 0.2 from Eqs. (4)–(5).

In order to investigate the role of ASSH in elastic modulus, θ_D of MGs and those of their solvent components are compared in Fig. 2. Interestingly, the θ_D values of these MGs are also almost equal to those of their solvent components. For instance, the θ_D of $(Fe_{0.9}Co_{0.1})_{72}B_{20}Si_4Nb_4$ MG is 480 K, which is nearly identical to that of pure polycrystalline Fe (470 K), and this value differs greatly from those of other components, i.e., Co (445 K), Cu (343 K), Si (645 K), and Nb (275 K). Therefore, one can conclude that the θ_D of MGs is primarily inherited from their solvent components.

It is well known that the spherelike clusters are efficiently packed to fill the space, and the ASSH also exits within the dense packed clusters in the microstructure of MGs. The cluster-formed glass also includes solutes that occupy the Einstein oscillator in the cluster assemblages and pin down the Debye oscillator vibration. The θ_D inheritance suggests a hierarchy of atomic bonding structure in MGs and their microstructure can be regarded as simple harmonic vibration model [7–9]. Then, the equivalent restoring force of interatomic bonds k_{MG} in MGs can be written as

$$k_{MG} = (1-f)k_D - \frac{1}{5}fk_D. \tag{6}$$

Moreover, the relationship between the restoring force of interactions (k) and Young's modulus (E) is given by $E = k / cd$, where d is the statistical average of interatomic distance on the first coordination shell in MGs and c is a constant [21,22]. Considering $k_E/k_D \approx 0.2$, Eq. (6) can be rewritten as

$$E_{MG} = \left[\frac{5(1-f)-f}{5}\right]E_{Sol} \tag{7}$$

where E_{MG} and E_{Sol} are Young's moduli of MG and solvent elements, respectively.

Similarly, the relationship between shear moduli G_{MG} and G_{Sol} for MG and solvent elements can be established using Young's modulus E by $E = 2.61G$ [23] as follows

$$G_{MG} = \left(1-\frac{6}{5}f\right)G_{Sol}. \tag{8}$$

It is known that the excess low frequency vibrations in the glass do not exist in crystalline materials, and it should be considered as a result of homogeneous structure, so we expect it should be related to the ASSH in MGs [5,11,12]. Thus, the calculated values and experimental results for other MG systems are also compared and listed in Table 2. It can be found that the calculations are very close to the experiments. The small deviation can be attributed to the variation of the bonding

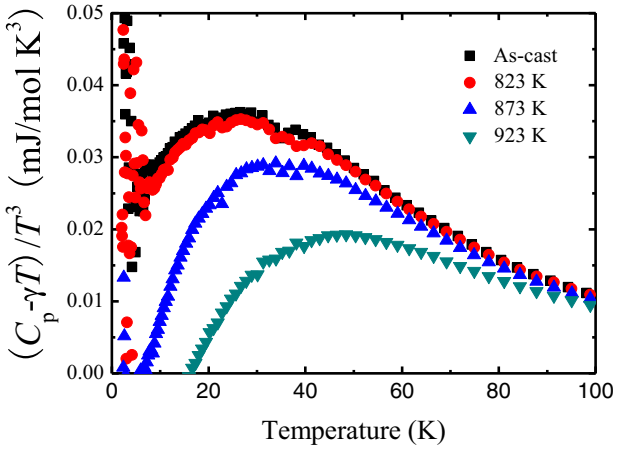

Fig. 3. Standard plotting of $(C_p - \gamma T) / T^3$ vs T of $Fe_{36}Co_{36}B_{20}Si_4Nb_4$ MG in the as-cast and annealed states. For clarity, only experimental data are shown.

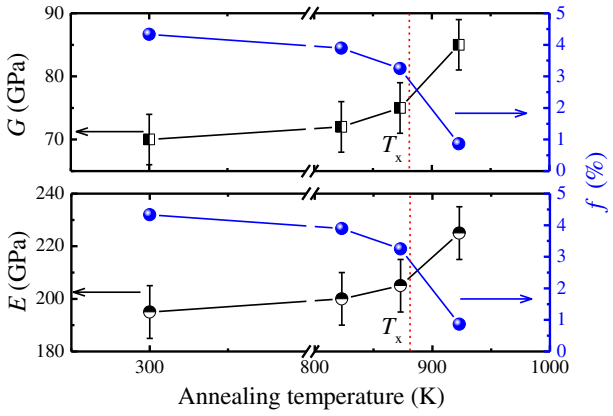

Fig. 4. (a) The fraction of ASSH and the shear modulus as a function of the annealing temperature. (b) The fraction of ASSH and the Young's modulus as a function of the annealing temperature. The curves are drawn as guides for the eye.

characteristics in the intercluster junctions, owing to either the presence of antisite solute atoms in the clusters leading to slightly tighter bonding [8], or some structural heterogeneity leading to looser bonding. Moreover, we can see that the different compositions of MGs have different values of f in Table 2. This is because the different addition of atoms with markedly different atomic sizes induces the change of the amount of the solute atoms and vacancies, and then the f is changed. Eqs. (7)–(8) can help us understand not only the elastic modulus inheritance [7–9], but also the elastic modulus sensitivity to the change of composition.

To further investigate the role of ASSH in the elastic modulus of MGs, the elastic modulus changes upon heat treatment during structure relaxation for $Fe_{36}Co_{36}B_{20}Si_4Nb_4$ MG are studied. Fig. 3 shows the standard plotting of $(C_p - \gamma T) / T^3$ vs T, it reveals an excess low frequency vibrations for $Fe_{36}Co_{36}B_{20}Si_4Nb_4$ MG after annealing. The amplitude of this peak has not been largely changed due to the structural relaxation at 823 K. Further annealing leads to a partial decrease in the peak, whether at 873 K or at higher temperatures (923 K). The fraction of ASSH f of $Fe_{36}Co_{36}B_{20}Si_4Nb_4$ MG during annealing is estimated from the excess peak data. Fig. 4 shows the dependence of the fraction f together with the elastic modulus E as a function of the annealing temperature. We can see that f becomes even lower after annealing near the crystallization temperature T_x, and it further reduces upon the crystallization of the MG. The structural relaxation anneals out upon heat treatment, so that ASSH almost vanishes in the crystalline state. This results in the increments of G and E with increasing f. The decreased ASSH is believed to increase the elastic modulus of MGs. The ASSH distributed region make it easier for a homogeneous generation of shear transformation zones within the entire specimen, which leads to a higher density of shear bands [6]. The E and G decrease due to the facilitated initiation of shear bands.

4. Conclusions

In this study, we estimate the fraction of ASSH in various MGs by using the localized vibrational model, and conclude that the change of elastic modulus of MGs can be attributed to the ASSH, which is considered as the basic entities responsible for corresponding change of elastic modulus. This study provides a useful microstructural insight into the origins of the correlation between structure and mechanical properties of MGs.

Acknowledgments

We would like to thank Shibu Saw, the University of Sydney (USYD) for his kind help and the corrections to this paper. We also appreciate insightful suggestions from the reviewers. This work is supported by the Fundamental Research Funds for the Central Universities (2014ZDPY35).

References

[1] J.Q. Wang, Y.H. Liu, M.W. Chen, G.Q. Xie, D.V. Louzguine-Luzgin, A. Inoue, J.H. Perepezko, Rapid degradation of Azo Dye by Fe-based metallic glass powder, Adv. Funct. Mater. 22 (2012) 2567–2570.
[2] Z.F. Yao, J.C. Qiao, C. Zhang, J.M. Pelletier, Y. Yao, Non-isothermal crystallization transformation kinetics analysis and isothermal crystallization kinetics in supercooled liquid region (SLR) of $(Ce_{0.72}Cu_{0.28})_{90-x}Al_{10}Fe_x$ (x = 0, 5 or 10) bulk metallic glasses, J. Non-Cryst. Solids 415 (2015) 42–50.
[3] W.M. Yang, H.S. Liu, Y.C. Zhao, A. Inoue, K.M. Jiang, J.T. Huo, H.B. Ling, Q. Li, B.L. Shen, Mechanical properties and structural features of novel Fe-based bulk metallic glasses with unprecedented plasticity, Sci. Rep. 4 (2014) 6233.
[4] W.M. Yang, H.S. Liu, C.C. Dun, J.W. Li, Y.C. Zhao, B.L. Shen, Nearly free electron model to glass-forming ability of multi-component metallic glasses, J. Non-Cryst. Solids 361 (2013) 82–85.
[5] H. Wagner, D. Bedorf, S. Kuchemann, M. Schwabe, B. Zhang, W. Arnold, K. Samwer, Local elastic properties of a metallic glass, Nat. Mater. 10 (2011) 439–442.
[6] H.W. Sheng, W.K. Luo, F.M. Alamgir, J.M. Bai, E. Ma, Atomic packing and short-to-medium range order in metallic glasses, Nature 439 (2006) 419–425.
[7] N. Zheng, R.T. Qu, S. Pauly, M. Calin, T. Gemming, Z.F. Zhang, J. Eckert, Design of ductile bulk metallic glasses by adding "soft" atoms, Appl. Phys. Lett. 100 (2012) 141901.
[8] D. Ma, A.D. Stoica, X.L. Wang, Z.P. Lu, B. Clausen, D.W. Brown, Elastic moduli inheritance and the weakest link in bulk metallic glasses, Phys. Rev. Lett. 108 (2012) 085501.
[9] W.H. Wang, Properties inheritance in metallic glasses, J. Appl. Phys. 111 (2012) 123519.
[10] J.Q. Wang, W.H. Wang, H.Y. Bai, Extended elastic model for flow in metallic glasses, J. Non-Cryst. Solids 357 (2011) 223–226.
[11] M.B. Tang, H.Y. Bai, M.X. Pan, D.Q. Zhao, W.H. Wang, Einstein oscillator in highly-random-packed bulk metallic glass, Appl. Phys. Lett. 86 (2005) 021910.
[12] Y. Li, H.Y. Bai, W.H. Wang, K. Samwer, Low-temperature specific-heat anomalies associated with the boson peak in CuZr-based bulk metallic glasses, Phys. Rev. B 74 (2006) 052201.
[13] S.V. Khonik, A.V. Granato, D.M. Joncich, A. Pompe, V.A. Khonik, Evidence of distributed interstitialcy-like relaxation of the shear modulus due to structural relaxation of metallic glasses, Phys. Rev. Lett. 100 (2008) 065501.
[14] K. Amiya, A. Urata, N. Nishiyama, A. Inoue, Magnetic properties of (Fe, Co)–B–Si–Nb bulk glassy alloys with high glass-forming ability, J. Appl. Phys. 97 (2005) 10F913-10F915.
[15] W.M. Yang, H.S. Liu, X.J. Liu, G.X. Chen, C.C. Dun, Y.C. Zhao, Q.K. Man, C.T. Chang, B.L. Shen, A. Inoue, R.W. Li, J.Z. Jiang, Correlation of atomic packing with the boson peak in amorphous alloys, J. Appl. Phys. 116 (2014) 123512.
[16] R. Kuentzler, D.E.G. Williams, Specific heat and structures of amorphous $Fe_{78-x}Co_xSi_{10}B_{12}$ alloys, J. Phys. F: Met. Phys. 15 (1985) 2283.
[17] M.B. Tang, H.Y. Bai, W.H. Wang, Tunneling states and localized mode in binary bulk metallic glass, Phys. Rev. B 72 (2005) 012202.
[18] C. Kittel, Introduction to Solid State Physics, 8th ed. Chemical Industry Press, Beijing, China, Chinese Ed., 2005. 86.
[19] H.S. Chen, W.H. Haemmerle, Excess specific heat of a glassy $Pd_{0.775}Cu_{0.06}Si_{0.165}$ alloy at low temperature, J. Non-Cryst. Solids 11 (1972) 161–169.
[20] W.M. Yang, H.S. Liu, X.Q. Yang, L.M. Dou, Low temperature specific heat of amorphous alloys, J. Low Temp. Phys. 160 (2010) 148–155.
[21] J.J. Mecholsky Jr., Estimating theoretical strength of brittle materials using fractal geometry, Mater. Lett. 60 (2006) 2485.
[22] C.C. Yuan, X.K. Xi, On the correlation of Young's modulus and the fracture strength of metallic glasses, J. Appl. Phys. 109 (2011) 033515.
[23] W.H. Wang, The elastic properties, elastic models and elastic perspectives of metallic glasses, Prog. Mater. Sci. 57 (2012) 487–656.
[24] J.J. Pang, M.J. Tan, K.M. Liew, On valence electron density, energy dissipation and plasticity of bulk metallic glasses, J. Alloys Compd. 557S (2013) S56–S65.
[25] A.N. Vasiliev, T.N. Voloshok, A.V. Granato, D.M. Joncich, Yu.P. Mitrofanov, V.A. Khonik, Relationship between low-temperature boson heat capacity peak and high-temperature shear modulus relaxation in a metallic glass, Phys. Rev. B 80 (2009) 172102.
[26] V.A. Khonik, Yu.P. Mitrofanov, S.A. Lyakhov, D.A. Khoviv, R.A. Konchakov, Recovery of relaxation in aged metallic glass as determined by high-precision in situ shear modulous measurements, J. Appl. Phys. 105 (2009) 123521.
[27] T. Wada, A. Inoue, A.L. Greer, Mechanical properties of porous bulk glassy alloy prepared in high-pressure hydrogen atmosphere, Mater. Sci. Eng. A 449 (2007) 958–961.